arXiv:cond-mat/0409750v1 [cond-mat.str-el] 29 Sep 2004

Field-Tuned Quantum Critical Point in $CeCoIn_5$ Near the Superconducting Upper Critical Field

F. Ronning,[1] C. Capan,[1] A. Bianchi,[2] R. Movshovich,[1] A. Lacerda,[3]
M. F. Hundley,[1] J. D. Thompson,[1] P. G. Pagliuso,[4] J. L. Sarrao[1]
[1]*Los Alamos National Laboratory, Los Alamos, New Mexico 87545*
[2]*Dresden High Magnetic Field Laboratory, Forschungszentrum Rossendorf, 01314 Dresden, Germany*
[3]*National High Magnetic Field Laboratory, Los Alamos, New Mexico 87545*
[4]*Instituto de Fisica Gleb Wataghin, UNICAMP, 13083-970, Campinas, Brazil*
(Dated: March 23, 2022)

We report a systematic study of high magnetic field specific heat and resistivity in single crystals of $CeCoIn_5$ for the field oriented in the basal plane (H‖ab) of this tetragonal heavy fermion superconductor. We observe a divergent electronic specific heat as well as an enhanced A coefficient of the T^2 law in resistivity at the lowest temperatures, as the field approaches the upper critical field of the superconducting transition. Together with the results for field along the tetragonal axis (H‖c), the emergent picture is that of a magnetic field tuned quantum critical point which exists in the vicinity of the superconducting H^0_{c2} despite a variation of a factor of 2.4 in H^0_{c2} for different field orientations. This suggests an underlying physical reason exists for the superconducting H^0_{c2} to coincide with the quantum critical field. Moreover, we show that the recovery of a Fermi Liquid ground state with increasing magnetic field is more gradual, meaning that the fluctuations responsible for the observed quantum critical phenomena are more robust with respect to magnetic field, when the magnetic field is applied in-plane. Together with the close proximity of the quantum critical point and H^0_{c2} in $CeCoIn_5$ for both field orientation, the anisotropy in the recovery of the Fermi liquid state might constitute an important piece of information in identifying the nature of the fluctuations that become critical.

PACS numbers:

Quantum critical points mark the change in the ground state of a strongly correlated electron system, and the associated quantum fluctuations have tremendous consequences for the properties of the system at finite temperatures. Attention has focused on the heavy fermion superconductor $CeCoIn_5$ in the context of quantum criticality since its discovery [1]. Superconductivity in this material is not only unconventional (probably *d*-wave [2, 3]) and Pauli-limited (with the possible presence of a Fulde-Ferrell-Larkin-Ovchinnikov state at low temperatures) [4, 5, 6] but it is also built out of a normal state displaying Non Fermi Liquid behavior. Indeed, the normal state is characterized by a resistivity almost linear in temperature for a decade above T_c in zero field [1], a specific heat coefficient diverging logarithmically over a large temperature range with a similar slope at zero and finite magnetic field [1, 7], and a power law behavior in ac-susceptibility [1, 7] and the nuclear spin-lattice relaxation rate [8]. All of this suggests the proximity to an antiferromagnetic instability. It is important to note that the specific heat is analogous to UBe_{13} [9]. Since the entropy is conserved between the zero field superconducting state and the anomalous normal state at H^0_{c2}, this implies that the mass enhancement leading to the heavy fermion ground state is interrupted by the formation of superconductivity and presumably the same spin fluctuations are responsible for both phenomena.

The phase diagram of $CeCoIn_5$ turns out to be rather complex, raising the possibility of one or more quantum critical points. On the one hand, under pressure the ground state evolves into a conventional Fermi Liquid, and the effective mass decreases, as evidenced by resistivity [10], specific heat [11], de Haas-van Alphen [12] and ^{115}In NQR measurements [13]. Moreover, the similarity in the pressure dependence of T_c in both $CeCoIn_5$ and the isostructural antiferromagnetic compound $CeRhIn_5$ points to the existence of a pressure-tuned antiferromagnetic quantum critical point close to ambient pressure in $CeCoIn_5$ [10].

On the other hand, systematic transport and thermodynamic investigations of the normal state at magnetic fields above $H^{\|c}_{c2} \simeq 5$ T [14, 15] have revealed that the ground state evolves into a Fermi Liquid with increasing field as well, meaning that pressure is not the only tuning parameter for $CeCoIn_5$. Moreover, for the same reasons as for the pressure phase diagram, one can speculate that the quantum critical point in the magnetic field phase diagram is an antiferromagnetic one. Surprisingly, the critical field is found to be close to the superconducting upper critical field H^0_{c2}. Although antiferromagnetic long range order has *not* been observed in $CeCoIn_5$, it has been suggested that it is avoided due to the formation of the superconducting ground state, and antiferromagnetic spin fluctuations may still be responsible for the observed quantum critical behavior at H^0_{c2} [15]. Since the superconducting transition itself is first order at low temperatures, possibly as a consequence of Pauli limiting [4, 5], it seemed natural to exclude the superconducting fluctuations from this picture. More recently,

a report of thermal conductivity above H_{c2}^0 showed a divergence in the scattering rate exactly identical to the one obtained from electrical resistivity, ruling out the possibility of superconducting fluctuations playing an important role in $CeCoIn_5$ [16]. On the other hand, a recent study on Sn-doped $CeCoIn_5$ shows that the superconducting upper critical field H_{c2}^0 is suppressed by Sn-doping exactly in the same manner as the quantum critical field [17], suggesting that the presence of a quantum critical point in the vicinity of H_{c2}^0 is *not* a coincidence in $CeCoIn_5$. It has also been pointed out in the pure compound that the quantum fluctuations result in a sub-linear temperature dependence in resistivity at finite fields, which is not well understood [16]. To date, the nature of the critical fluctuations at H_{c2}^0 is still not established despite considerable efforts and it adds yet another mystery to the intimate relationship between antiferromagnetism and superconductivity in the 115 family.

All the above-mentioned work related to quantum critical phenomena at finite fields has been performed with the magnetic field applied *parallel* to the tetragonal c-axis, which is the easy axis of magnetization in the 115 family. Since the upper critical field is anisotropic, it is important to check if the phase diagram is similar when the field is applied in the basal plane, i.e. whether the quantum critical behavior is tied to the destruction of superconductivity at H_{c2}. This is precisely the motivation of this work. We measured specific heat and resistivity in single crystals of $CeCoIn_5$ for magnetic fields *perpendicular* to the c-axis, ranging between 12 T and 18 T and temperatures between 50 mK and 3 K, in the 20 T magnet at the National High Magnetic Field Laboratory, using a dilution refrigerator. Specific heat is measured in the same single crystal for both field orientations, with a quasi-adiabatic heat pulse technique, so that we can compare this data against the specific heat data for H‖c from ref. [15]. Resistivity is measured in a second single crystal, of good quality and geometry, with no free In, having a RRR ratio of 111 with a residual resistivity of 0.3 $\mu\Omega$.cm with H‖ab. The contacts are made by spotwelding Pt wires with a geometry such that J⊥H and J,H‖ab, and care was taken to ensure that there is no self-heating in the sample created by current at the lowest temperatures. Both specific heat and resistivity results for the in-plane orientation show a magnetic field-tuned quantum critical point in the vicinity of the upper critical field $H_{c2}^{\|ab} \simeq 11.8$ T, similar to the c-axis results, even though the upper critical field has increased by a factor of 2.4 as compared to the c-axis. Moreover, we show that the magnetic field is less effective in suppressing the critical fluctuations and restoring the Fermi Liquid behavior in this orientation, as compared to H‖c. This is in contrast to the behavior observed in tetragonal $YbRh_2Si_2$, which is an example of a field tuned antiferromagnetic quantum critical point. For $YbRh_2Si_2$, the evolution of the Fermi temperature determined from

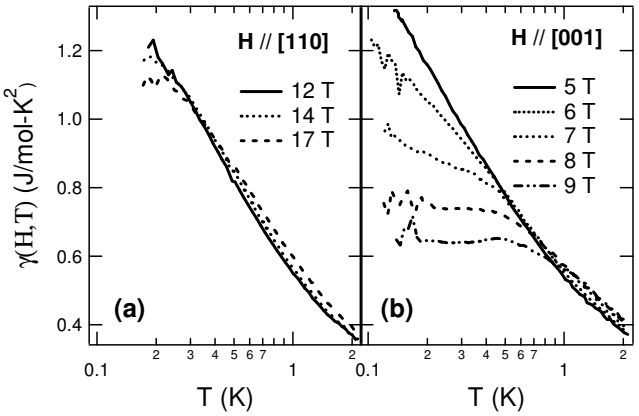


FIG. 1: The Sommerfeld coefficient of the electronic specific heat as a function of temperature for magnetic fields above H_{c2}^0 oriented in the plane (left panel) and parallel to c-axis (right panel) on the same crystal. The evolution from NFL to FL behavior with increasing field is more gradual when the field is oriented in-plane. The data for H‖c is from ref. [15].

resistivity as well as the divergence of the T^2 term in resistivity as a function of the reduced field are roughly the same for the two field orientations [18]. Although the anisotropy factor in the critical field of $CeCoIn_5$(2.4) is much smaller than $YbRh_2Si_2$(11), our results show that the effective "distance" to the quantum critical point depends on the orientation of the magnetic field. In light of these observations, more theoretical work is needed to better understand the nature of the field-tuned quantum critical point in $CeCoIn_5$.

Figure 1 shows the electronic specific heat coefficient $\gamma \equiv C_{el}/T$ in the normal state as a function of temperature, on a semi-logarithmic scale, for the magnetic field oriented in the plane (left panel) and parallel to the c-axis (right panel) in the same single crystal. The electronic contribution is obtained after subtraction of the nuclear Schottky and lattice contributions from the measured specific heat [2]. In both orientations, the specific heat is divergent down to the lowest measured temperature at H≈H_{c2} which is 4.95 T and 11.8 T respectively for field parallel and perpendicular to the c-axis. Moreover, the two curves at these fields overlap almost perfectly in the whole temperature range for the two orientations. However, the evolution of the specific heat as the magnetic field is increased above H_{c2} depends on the field orientation. For magnetic fields in the plane, the specific heat is barely changed over the entire temperature range when the field is increased up to 17 T, corresponding to a 44% relative increase above the critical field. Both 14 T and 17 T curves show essentially a diverging specific heat as the temperature decreases, corresponding to Non Fermi Liquid behavior. Only at 17 T a crossover to a Fermi Liquid regime, characterized by a constant γ, can be resolved around 0.2 K, with a γ(0.2 K) value reduced to 1.1 J/molK^2, only 8% less than its 0.2 K value at

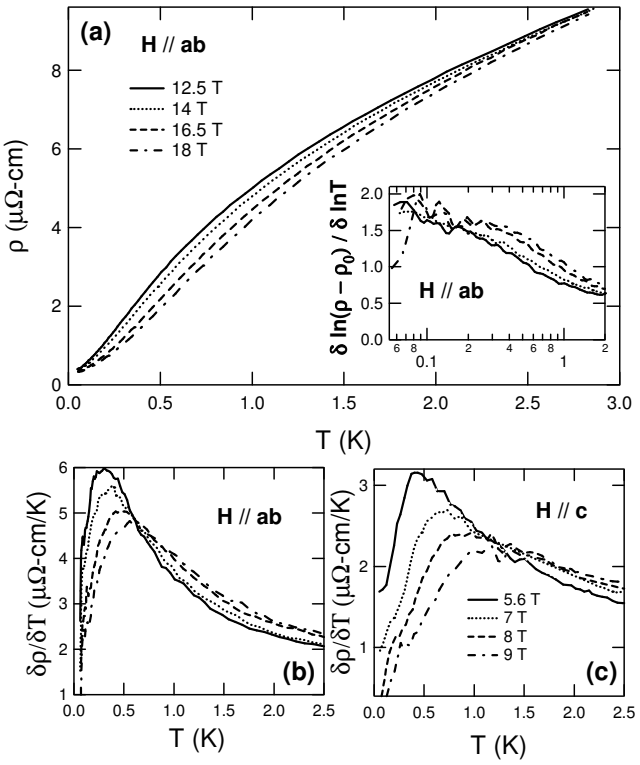


FIG. 2: (a) Resistivity as a function of temperature between 50 mK and 3 K for magnetic fields up to 18 T oriented in the plane. Inset: the same data is shown as a semi-log plot of the effective exponent of resistivity as a function of temperature, defined as the logarithmic derivative of $\rho - \rho_0$. Note that the asymptotic value at high temperatures is less than 1. The maximum in $\frac{\delta\rho}{\delta T}$ for H‖ab (panel b) and H‖c (panel c) tracks the inflection point in resistivity, from which one can see that the field has a significantly greater effect when applied along the c-axis.

H_{c2}. In contrast, when the field is along the c-axis, the effect of the field is stronger and the divergence of the specific heat is more easily suppressed as the field is increased. For a comparable relative change in field of 41%, corresponding to H = 7 T in this orientation, γ(0.2 K) is readily suppressed to 0.9 J/mol K^2 which is 25% less than its value at H_{c2} for the same temperature of 0.2 K. With further increasing magnetic field in the c-axis orientation, the specific heat tends to saturate at low temperatures and a clear Fermi Liquid regime extends up to 0.5 K at the highest field of 9 T as was reported in ref. [15].

Resistivity as a function of temperature in a separate single crystal measured between 50 mK and 3 K with magnetic fields applied in-plane, from 12.5 T to 18 T is shown in figure 2(a). Electric current was applied in-plane but perpendicular to the field. The overall S-shape of the resistivity seen on the upper panel in this orientation is qualitatively similar to the c-axis data published previously [14, 15]. In the low temperature limit the curvature of resistivity is upward and the negative magnetoresistance is significant, in contrast to the high temperature regime where the curvature becomes negative and the magnetoresistance is reduced. Despite the qualitative similarities in the overall shape of ρ for H‖c and H‖ab, there is a striking difference in the rate of evolution as a function of field between the two orientations. This can be characterized by the temperature T^* of the inflection point in resistivity versus temperature, which will appear as a maximum in $\frac{\delta\rho}{\delta T}$. Obviously these temperatures are larger than the temperatures up to which the Fermi Liquid behavior extends. Nevertheless, T^* can be taken as a crossover between the low temperature Fermi Liquid regime and high temperature Non Fermi Liquid regime, as in the case of $YbRh_2Si_2$ [19]. Figures 2(b) and 2(c) show that the temperature of the inflection point rises much more rapidly with increasing field for H‖c than for H‖ab.

The inset of figure 2(a) presents the logarithmic derivative of $\Delta\rho = \rho - \rho_0$ with respect to temperature, as a function of temperature. The evolution of this effective exponent is worth a few comments. First, in a temperature range which is dominated by quantum critical fluctuations as evidenced by the observed scaling in refs. [15] and [16], the exponent saturates to a value less than 1 in the high temperature limit, independent of the field. This is consistent with the 2/3 exponent in this temperature range reported for field along the c-axis at finite fields [16]. Second, the value of 2 corresponding to Fermi Liquid regime is only reached in the limit of low temperatures, with an onset temperature increasing slightly with field. In the intermediate temperature range, one observes a plateau around the value of 3/2 which becomes more extended in temperature as the field is increased. The overall shape of the logarithmic derivative is reminiscent of the theoretical curves from ref. [20] in the framework of a spin density wave scenario, and, in general, emphasizes that there is no universal, single power law temperature dependence in the Non Fermi Liquid behavior of resistivity.

The fact that the in-plane resistivity can be fitted with a quadratic $\rho = \rho_0 + AT^2$ law only at the lowest temperatures is shown in the upper panel of figure 3, corresponding to a Fermi Liquid regime over a rather limited temperature range. This is consistent with Non Fermi Liquid behavior in the specific heat data extending over a large temperature range for the in-plane orientation, as described above. As the magnetic field increases from 12.5 T to 18 T, the A coefficient corresponding to the slope of the T^2 behavior is significantly reduced. At the same time, the temperature up to which the T^2 fit holds, defining the Fermi temperature obtained from resistivity, increases slightly but systematically [21]. The magnetic field dependence of the A coefficient and the Fermi temperature are displayed in figure 3(b) and 4, respectively. Both the enhancement of the A coefficient

and the decrease in the Fermi temperature are consistent with the specific heat diverging to lower temperatures as the field approaches the superconducting upper critical field. This suggests the presence of a field-tuned quantum critical point in the vicinity of H_{c2} for field in-plane orientation. A similar conclusion has been drawn in the previous reports for field along the c-axis [14, 15]. Thus, our results imply that the quantum critical point has the same anisotropy as the superconducting upper critical field.

Despite the analogy between the two field orientations, one notices a quantitative difference when comparing the rate at which the magnetic field tunes the system into a Non Fermi liquid regime. Not only is the Fermi Liquid regime restricted to a smaller portion of the phase diagram but the rise of the Fermi temperature as the field increases above H_{c2} is more gradual for the in-plane orientation, as shown in figure 4. This is also directly seen in the difference between resistivity for field in-plane (at 12.5 T and 18 T) and for field along the c-axis (at 6 T and 9 T) again in the same crystal, as shown in the inset of figure 3 (a). Clearly, the quadratic temperature dependence of resistivity has a stronger slope, when the field is in-plane, but the data deviates from T^2 law at a much lower temperature than the c-axis data. The difference in the A coefficient for the two field orientations is shown in figure 3 (b). We have compiled the results of the T^2 fits from various samples for comparison, and present the A coefficient as a function of the reduced field $\frac{H-H_{c2}}{H_{c2}}$ for the two orientations (with $H_{c2}^{\|ab} = 11.8$ T and $H_{c2}^{\|c} = 4.95$ T). Included in figure 3 are results from data in figure 2, with the magnetic field applied parallel and perpendicular to the c-axis in the same crystal, as are results from previously published data for H‖c from ref. [14, 15]. Moreover, we have included results from longitudinal magnetoresistance data, with field parallel to the current and parallel to the plane (raw data not shown). We find that the field in-plane A coefficient is systematically larger than the c-axis one, but it is less divergent as well, beyond sample-to-sample variations. The residual resistivity also has a different evolution depending on the field orientation. The inset of figure 3 (b) shows that the residual resistivity is almost constant as a function of the reduced field, when field is applied in the plane, but it is strongly increasing when field is along the c-axis in the same single crystal.

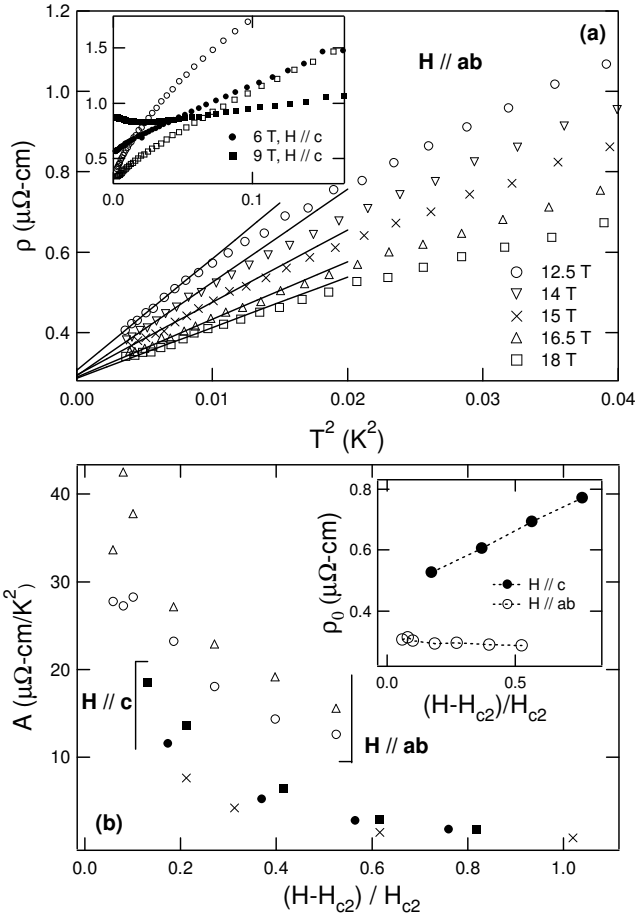


FIG. 3: (a) Resistivity vs. T^2 at low temperatures for H‖ab. The symbols represent data between 12.5 T and 18 T as indicated in the figure and the solid lines represent the T^2 fit. The inset shows the 12.5 T and 18 T data for field in-plane (open symbols) together with 6 T and 9 T data for field along the c-axis (filled symbols) in the same single crystal for comparison. Note the larger slope and smaller temperature range for the T^2 behavior in resistivity when the field is in-plane. (b) Coefficient A as a function of reduced field $\frac{H-H_{c2}}{H_{c2}}$ obtained from the $\rho = \rho_0 + AT^2$ fits for field parallel (filled symbols) and perpendicular (open symbols) to the c-axis. The open (○) and closed (●) circles correspond to the data on the same sample. The inset of the lower panel shows the residual resistivity ρ_0 vs. reduced field for both orientations for the same sample. In the main panel: △ corresponds to a second sample measured with field in-plane and parallel to the electric current, ■ is for the sample of Ref. [15] and × is taken from Ref. [14] both with field parallel to the c-axis. All data have current in the plane. Note that the A coefficient for field in-plane is larger than the A coefficient for field along the c-axis.

At this point, a word of caution regarding the analysis of the resistivity data is in order. It is by no means clear that the data down to 50 mK has saturated to its limiting T^2 behavior. This becomes even more likely as the field approaches H_{c2}, and the already limited range for T^2 behavior systematically shrinks. An additional problem for the determination of the A coefficient for H‖c can be due to the low temperature upturn in resistivity. Even though we exclude this portion of the data from the fits, the values are still underestimated when compared to the sample of ref. [15] where no upturn was present. A similar upturn has also been reported in ref. [14] and was presumed to be a Fermi surface effect involving closed orbits when the quantum limit is reached. This is consistent with the two dimensional nature of parts of the Fermi surface, as we do not observe

the upturn in the same sample when the magnetic field is in-plane, twice as large, and still perpendicular to the current, rather only for H‖c, as shown in the inset of figure 3 (a). The trend in the c-axis data is that the upturn becomes more pronounced and starts at a higher temperature as the field increases, and the values are consistent with the $\omega_c\tau = 1$ condition [22]. So it is quite possible that the reported A values may be lower bounds, which is why we have refrained from quantitatively fitting the divergences. However, it is clear that potential corrections, were we able to measure to lower temperatures, would only increase the divergence of A, thus making the case for the field tuned-quantum critical point to lie at the superconducting H_{c2} even stronger.

We should also stress that the uncertainties related to the analysis do not compromise the validity of the points we emphasize. The inset of figure 3 (a) shows that there is indeed substantially more scattering when the field is oriented in the plane. Our determination of the A coefficient, which suggests a quantum critical point at the superconducting H_{c2}, is corroborated by a log(T) divergence in C/T at H_{c2} down to the lowest temperatures measured by specific heat. Furthermore, the fact that the non-Fermi liquid regime is more robust when the field is applied in the plane is seen clearly both in the specific heat data of figure 1 and in tracking the inflection point in the resistivity curves in figure 2.

In trying to understand our data, it is constructive to first consider the effect of the Fermi surface topology. de Haas-van Alphen (dHvA) measurements reveal that the Fermi surface of $CeCoIn_5$ has large 2-dimensional surfaces as well as small 3-dimensional pockets [23, 24]. If the conductivity is dominated by the 2-dimensional surfaces one would expect an orbital component to the magnetoresistance which is always positive when the field is along the c-axis (closed orbits), and field independent with H‖ab (open orbits) [25]. Indeed, this explains why the residual resistivity has a positive field dependence for H‖c, and none for H‖ab. The field-independent in-plane residual resistivity further suggests that the elastic scattering from disorder is not affected by the strong fluctuations leading to the large mass enhancement. At finite temperatures the negative magnetoresistance is accounted for by the suppression of quantum fluctuations (and hence the A coefficient) as one moves away from the quantum critical point. This is also seen in dHvA by the reduction of the effective mass of the 2-dimensional sheets as the field is increased beyond H_{c2} with H‖c [23]. The fact that the masses of the 3-dimensional pockets are significantly less enhanced as the critical field is approached suggests that transport with the current along the c-axis should be markedly different [26]. Unfortunately, dHvA is blind to the 2 dimensional sheets when the field is oriented in the plane, and so it can not compare the relative mass enhancement for the two field orientations as we have done here. Moreover, the anisotropy of the spin fluctuations with respect to the field orientation is yet to be established by a direct probe like NMR or neutron scattering.

Can an anisotropic g-factor, which represents the effective coupling between the magnetic excitations and the external field, explain the observed anisotropy in the scattering rates? By fitting the H_{c2}(T) curves Maki *et al.* found g values of 1.5 and 0.64 for H‖c and H‖ab, respectively which is nearly identical to the ratio of H_{c2} for the two field orientations [27]. Thus, we have attempted to take into account the anisotropy in the g-factor (and in H_{c2}) by plotting the data against a renormalized H. The phase diagram as a function of temperature and reduced field ($\frac{H}{H_{c2}}$), shown in figure 4, nearly accounts for the anisotropy in the inflection point of the resistivity curves. However, it does not account for the anisotropy in A(H) from figure 3 (b). Accounting for different g-factors, close to a critical point one expects the A coefficient to diverge as $A(H) = A_0\ (\frac{H-H_{c2}}{H_{c2}})^{\alpha}$. Figure 3 (b) would then lead us to conclude that $A_0^{H\|ab} \approx 3A_0^{H\|c}$. In addition, the Fermi temperature anisotropy is also not accounted for in this way. While the values for H‖ab may simply represent upper limits, the values for H‖c of 8 T and 9 T are well established by both specific heat and resistivity. Thus we can see that for $\frac{H}{H_{c2}} > 1.5$, $T_F^{\|ab}$ is less than half $T_F^{\|c}$. This is also consistent with our discussion of the anisotropy in the specific heat data of figure 1. Thus, we conclude that the quantum fluctuations are significantly more robust when the field is applied in the plane, and that the origin of this anisotropy is not solely a result of an anisotropic g-factor.

At this point, we consider how our data impact the various quantum critical point scenarios for $CeCoIn_5$. One possibility is that the quantum critical behavior originates from the second superconducting phase which was identified for H‖ab [5]. Although the inflection point in the resistivity curves appear to originate from this phase boundary for H‖ab, there is no other data which ties this phase transition to the quantum critical behavior. In addition, for H‖c the inflection point in resistivity has nearly identical behavior to H‖ab, while a second superconducting transition is strongly suppressed for this orientation [5]. Thus we can confidently rule out this origin for the quantum critical behavior.

Why is the quantum critical field tied so closely to the superconducting H_{c2}? We now believe this to be more than a mere coincidence since attempts to separate one from the other with either Sn doping [17] or field orientation (more than a factor of 4 change in H_{c2} combined) could not do so. Thus, it would appear that the quantum critical behavior originates from a superconductor to paramagnet quantum phase transition. However, the width of the fluctuation regime for a BCS

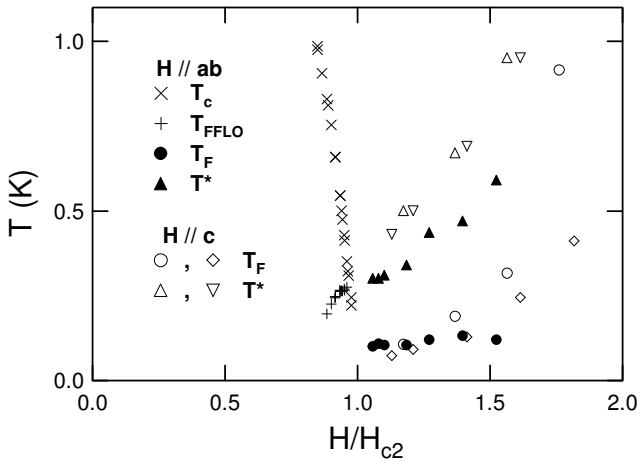


FIG. 4: H-T phase diagram of $CeCoIn_5$ on a reduced scale for both H‖c and H‖ab orientations. The superconducting upper critical field is obtained from previous specific heat measurements of ref. [4, 5], T_F was determined from the T^2 resistivity fits, and T^* is the inflection point in resistivity versus temperature. T_F and T^* for H‖ab are from the same sample whose data for H‖c are shown with ∘ and △ respectively. Symbols ◇ and ▽ are obtained from data presented in ref. [15]

superconductor is extremely small, even for nodal superconductors, and can be approximated by the Ginzburg criteria to be $\Delta T/T_c = [(2\pi\xi_0)^{-3}k_B/\Delta C]^2 \approx 10^{-9}$ for $CeCoIn_5$. Disorder can increase this fluctuation regime by pair breaking effects possibly leading to a quantum critical point as shown in ref. [28], but we would not expect this to apply to the extremely pure system of $CeCoIn_5$. Further, we note that the superconducting $H_{c2}(T)$ boundary as $T \to 0$ is first order [4]. Thus it would require a truly novel type of superconductor to produce the observed quantum critical point. An alternative view is that the quantum criticality in this system originates from an antiferromagnetic quantum critical point. Then the correct question to ask is why is the superconducting H_{c2} tied to the quantum critical point? This could be possible if the low field phase had a large susceptibility to become superconducting. Superconductivity is then destroyed at the quantum phase transition since the susceptibility to superconductivity in the high-field phase is significantly lower. This is precisely what has been observed theoretically in low density systems [29]. In principle the quantum critical point could separate any two ground states, but comparing $CeCoIn_5$ to $CeRhIn_5$ suggests that the quantum critical point separates an antiferromagnetic ground state from a high field paramagnetic state. For the case of an antiferromagnetic quantum critical point we might also expect to find short range antiferromagnetic order inside the vortex cores below H_{c2}.

In conclusion, we have measured specific heat and resistivity in $CeCoIn_5$ with H‖ab. The specific heat shows $C/T \propto \log(T)$ down to the lowest temperature measured at $H_{c2} \simeq 12$ T. Resistivity measurements also show that the electron-electron scattering diverges at H_{c2}, and that at high temperatures the resistivity has a sub-linear power law. Thus, for both field orientation there is a field-tuned quantum critical point close to H_{c2}, but the Fermi temperature is smaller and the tuning much slower for the field in-plane orientation. This means that the magnetic field is more efficient in suppressing the heavy fermion ground state in the c-axis orientation. The fact that it is experimentally impossible to distinguish the quantum critical point from the upper critical field independent of field orientation must be a consequence of a common underlying mechanism for both phenomena. The origin of the anisotropy in the tuning rate with respect to the field orientation might provide a clue to the nature of the fluctuations that become critical at H_{c2}.

Acknowledgments

We acknowledge fruitful discussions with A. Abanov, E.D. Bauer, N. Curro, A. Millis, A. Rosch, A. Schofield, and I. Vekhter. F.R. thanks the Reines Postdoctoral Fellowship (DOE-LANL) for support. Work at Los Alamos National Laboratory was performed under the auspices of the U.S. Department of Energy. Work at the NHMFL was performed under the auspices of the National Science Foundation, the State of Florida and the US Department of Energy.

[1] C. Petrovic, P.G. Pagliuso, M.F. Hundley, R. Movshovich, J.L. Sarrao, J.D. Thompson, Z. Fisk, P. Monthoux, J. Phys. Cond. Mat. **13**, L337 (2001).
[2] R. Movshovich, M. Jaime, J.D. Thompson, C. Petrovic, Z. Fisk, P.G. Pagliuso, J.L. Sarrao, Phys. Rev. Lett. **86**, 5152 (2001).
[3] K. Izawa, H. Yamaguchi, Y. Matsuda, H. Shishido, R. Settai, Y. Onuki, Phys. Rev. Lett. **87**, 057002 (2001).
[4] A. Bianchi, R. Movshovich, N. Oeschler, P. Gegenwart, F. Steglich, J.D. Thompson, P.G. Pagliuso, J.L. Sarrao, Phys. Rev. Lett. **89**, 137002 (2002).
[5] A. Bianchi, R. Movshovich, C. Capan, P.G. Pagliuso, J.L. Sarrao, Phys. Rev. Lett. **91**, 187004 (2003).
[6] H.A. Radovan, N.A. Forture, T.P. Murphy, S.T. Hannahs, E.C. Palm, S.W. Tozer, D Hall, Nature **425**, 51 (2003).
[7] J.S. Kim, J. Alwood, G.R. Stewart, J.L. Sarrao, J.D. Thompson, Phys. Rev. B **64**, 134524 (2001).
[8] Y. Kohori, Y. Yamato, Y. Iwamoto, T. Kohara, E.D. Bauer, M.B. Maple, J.L. Sarrao, Phys. Rev. B **64**, 134526 (2001).
[9] H.R. Ott, H. Rudigier, T.M. Rice, K. Ueda, Z. Fisk, J.L.

Smith, Phys. Rev. Lett. **52**, 1915 (1984).
[10] V.A. Sidorov, M. Nicklas, P.G. Pagliuso, J.L. Sarrao, Y. Bang, A.V. Balatsky, J.D. Thompson, Phys. Rev. Lett. **89**, 157004 (2002).
[11] G. Sparn, R. Borth, E. Lengyel, P.G. Pagliuso, J.L. Sarrao, F. Steglich, J.D. Thompson Physica B **319**, 262 (2002).
[12] H. Shishido, T. Ueda, S. Hashimoto, T. Kubo, R. Settai, H. Harima, Y. Onuki, J. Phys. Cond. Mat. **15**, L499 (2003).
[13] Y. Kohori, H. Saito, Y. Kobayashi, H. Taira, Y. Iwamoto, T. Kohara, T. Matsumoto, E.D. Bauer, M.B. Maple, J.L. Sarrao, J. Mag. Mag. Mat. **272-276**, 189 (2004).
[14] J. Paglione, M.A. Tanatar, D.G. Hawthorn, E. Boaknin, R.W. Hill, F. Ronning, M. Sutherland, L. Taillefer, C. Petrovic, P.C. Canfield, Phys. Rev. Lett. **91**, 246405 (2003).
[15] A. Bianchi, R. Movshovich, I. Vekhter, P.G. Pagliuso, J.L. Sarrao, Phys. Rev. Lett. **91**, 257001 (2003).
[16] J. Paglione, M.A. Tanatar, D.G. Hawthorn, E. Boaknin, R.W. Hill, F. Ronning, M. Sutherland, L. Taillefer, C. Petrovic, P.C. Canfield, **cond-mat**/0405157 (2004).
[17] E.D. Bauer, C. Capan, F. Ronning, R. Movshovich, J.D. Thompson, J.L. Sarrao, **cond-mat**/0409559 (2004).
[18] P. Gegenwart, J. Custers, C. Geibel, K. Neumaier, T. Tayama, K. Tenya, O. Trovarelli, F. Steglich, Phys. Rev. Lett. **89**, 056402 (2002).
[19] J. Custers, P. Gegenwart, H. Wilhelm, K. Neumaier, Y. Tokiwa, O. Trovarelli, C. Geibel, F. Steglich, C. Pepin, P. Coleman, Nature **424**, 504 (2003).
[20] A. Rosch, Phys. Rev. B **62**, 4945 (2000).
[21] T_F was defined as the temperature at which there was a 2% deviation of the data from the T^2 fit.
[22] If we let $\omega_c = \frac{eH}{m^*c}$, $\tau = \frac{m^*}{ne^2\rho}$, and $n = 6.2 \times 10^{27}\ m^{-3}$ for $CeCoIn_5$ then $\omega_c\tau = 1$ implies $\rho[\mu\Omega.cm] = 0.1010199 \times H[\mathrm{T}]$. For 7 T and 9 T this gives $\rho \simeq 0.7\mu\Omega.cm$ and $\rho \simeq 0.9\mu\Omega.cm$ respectively, which is in good agreement with the experimental value of the resistivity minimum in the H||c orientation.
[23] R. Settai, H. Shishido, S. Ikeda, Y. Murakawa, M. Nakashima, D. Aoki, Y. Haga, H. Harima, Y. Onuki, J. Phys. Cond. Mat. **13**, L627 (2001).
[24] D. Hall, E.C. Palm, T.P. Murphy, S.W. Tozer, Z. Fisk, U. Alver, R.G. Goodrich, J.L. Sarrao, P.G. Pagliuso, T. Ebihara, Phys. Rev. B **64**, 212508 (2001).
[25] C.M. Hurd, Hall Effect in Metals and Alloys (1972).
[26] A. Malinowski, unpublished.
[27] H. Won, K. Maki, S. Haas, N. Oeschler, F. Weickert, P. Gegenwart, Phys. Rev. B **69**, 180504(R) (2004).
[28] R. Ramazashvili, P. Coleman, Phys. Rev. Lett. **79**, 3752 (1997).
[29] P.C. Howell, A.J. Schofield, **cond-mat**/0103191 (2001).